Reactive oxygen species induce epithelial-mesenchymal transition, glycolytic switch, and mitochondrial repression through the Dlx-2/Snail signaling pathways in MCF-7 cells

SU YEON LEE[1*], MIN KYUNG JU[1*], HYUN MIN JEON[1,4*], YIG JI LEE[1], CHO HEE KIM[1,5], HYE GYEONG PARK[2], SONG IY HAN[3] and HO SUNG KANG[1]

[1]Department of Molecular Biology, College of Natural Sciences;
[2]Nanobiotechnology Center, Pusan National University, Busan 46241;
[3]Division of Natural Medical Sciences, College of Health Science, Chosun University, Gwangju, Gyeonggi 61452, Republic of Korea

Received September 20, 2018; Accepted March 20, 2019

DOI: 10.3892/mmr.2019.10466

Abstract. Reactive oxygen species (ROS) are important cellular second messengers involved in various aspects of cell signaling. ROS are elevated in multiple types of cancer cells, and this elevation is known to be involved in pathological processes of cancer. Although high levels of ROS exert cytotoxic effects on cancer cells, low levels of ROS stimulate cell proliferation and survival by inducing several pro-survival signaling pathways. In addition, ROS have been shown to induce epithelial-mesenchymal transition (EMT), which is essential for the initiation of metastasis. However, the precise mechanism of ROS-induced EMT remains to be elucidated. In the present study, it was indicated that ROS induce EMT by activating Snail expression, which then represses E-cadherin expression in MCF-7 cells. It was further indicated that distal-less homeobox-2 (Dlx-2), one of the human Dlx gene family proteins involved in embryonic development, acts as an upstream regulator of ROS-induced Snail expression. It was also revealed that ROS treatment induces the glycolytic switch, a phenomenon whereby cancer cells primarily rely on glycolysis instead of mitochondrial oxidative phosphorylation for ATP production, even in the presence of oxygen. In addition, ROS inhibited oxidative phosphorylation and caused cytochrome c oxidase inhibition via the Dlx-2/Snail cascade. These results suggest that ROS induce EMT, the glycolytic switch and mitochondrial repression by activating the Dlx-2/Snail axis, thereby playing crucial roles in MCF-7 cancer cell progression.

Correspondence to: Dr Ho Sung Kang, Department of Molecular Biology, College of Natural Sciences, Pusan National University, 2 Busandaehak-ro 63beon-gil, Geumjeong-gu, Busan 46241, Republic of Korea
E-mail: hspkang@pusan.ac.kr

Present addresses: [4]Department of Internal Medicine and Institute of Health Science, Gyeongsang National University School of Medicine and Hospital, Jinju-si, Gyeongnam 52828; [5]DNA Identification Center, National Forensic Service, Wonju-si, Gangwon-do, 26460, Republic of Korea

[*]Contributed equally

Key words: reactive oxygen species, epithelial-mesenchymal transition, glycolytic switch, Snail, distal-less homeobox 2

Introduction

Reactive oxygen species (ROS) are crucial cellular secondary messengers involved in diverse biological processes in cancer cells (1-7). ROS are oxygen-containing species, including superoxide ($O_2^{\bullet-}$), hydroxyl ($^{\bullet}OH$), and hydrogen peroxide (H_2O_2). The majority of ROS are produced as side products of oxidative phosphorylation in mitochondria (4,5,8,9), but they are also induced by NADPH oxidase (NOX), growth factors, and cytokines (2,4). ROS are increased in many types of cancers and these elevated ROS are highly involved in tumor development and progression (2,6,10). High levels of ROS exert cytotoxic effects by inducing DNA damage or cell death, thereby limiting cancer progression (2,4,5,7). On the other hand, at low levels, ROS function as signaling molecules that can induce nucleic acid and protein synthesis, cell cycle progression, the expression of numerous genes involved in cell proliferation and survival, the activation of redox-sensitive transcription factors [such as p53, hypoxia inducible factor (HIF)-1, and NF-κB], epigenetic alterations, and tumorigenesis (2,4,5,7). In addition, ROS have been shown to induce epithelial-mesenchymal transition (EMT) in cancer cells (11-14). However, the precise mechanism of ROS-induced EMT remains to be elucidated.

EMT plays critical roles in embryogenesis as well as in tumor invasion and metastasis. Epithelial cells undergoing EMT lose their polarization and acquire mesenchymal-like morphology. EMT is also characterized by decreased expression of epithelial markers, such as E-cadherin and induction of mesenchymal markers, such as vimentin. Loss of E-cadherin is considered a hallmark of EMT (15-19). EMT

is regulated by several transcription factors, including Snail, Slug, Twist-related protein (Twist)1, Twist2, zinc finger E-box binding homeobox (ZEB)1, ZEB2, and E12/E47. Snail, a key transcription factor in EMT, promotes invasion and metastasis in response to several oncogenic signaling pathways (20-22). Recently, Snail has been implicated in metabolic alterations, such as glycolytic switch (21,23). Glycolytic switch is a phenomenon whereby cancer cells rely on glycolysis more than mitochondrial oxidative phosphorylation for ATP production, even when sufficient oxygen is available (24-28). Recently, we showed that distal-less homeobox-2 (Dlx-2) induces EMT and glycolytic switch by activating Snail (29,30). Dlx-2 is one of the human distal-less (Dlx) gene family proteins and is involved in embryonic development (31,32) and tumor progression (33-36). Dlx-2 is known to play an important role in shifting the activity of TGF-β from tumor suppression to tumor promotion (34).

In this study, we show that ROS induce EMT through Snail and Dlx-2 cascades. We also show that Dlx-2/Snail signaling plays a critical role(s) in ROS-induced glycolytic switch, inhibition of mitochondrial respiration, and cytochrome c oxidase (COX) inhibition. These results clarify the mechanism by which ROS promotes tumor progression through Dlx-2/Snail axis-dependent EMT and glycolytic switch in MCF-7 cells.

Materials and methods

Cell culture and ROS treatment. MCF-7 cells were obtained from the American Type Culture Collection (ATCC, Manassas, VA, USA; authenticated by short tandem repeat profiling). MCF-7 cells were cultured in Eagle's minimal essential medium (EMEM; Hyclone; GE Healthcare, Logan, UT, USA) supplemented with 10% (v/v) heat-inactivated fetal bovine serum (FBS, Hyclone; GE Healthcare) and 1% penicillin-streptomycin (PS, Hyclone; GE Healthcare). Cells were cultured at 37˚C in a humidified incubator with 5% CO_2 and were passaged two times per week. Low-passage cultures (passage 5-25) were used for all experiments. Cells were routinely checked for mycoplasma contamination using the Mycoplasma PCR Detection kit (iNtRON Biotechnology). MCF-7 cells were treated with ROS [200 μM H_2O_2 (Sigma-Aldrich, St. Louis, MO, USA) and 10 μM menadione (an O_2^- generator; Sigma)].

Transfection and short hairpin RNA (shRNA) interference. pCR3.1-Snail-Flg (provided by J.I. Yook, Yonsei University, Korea) was transfected into MCF-7 cells using jetPEI (Polyplus-transfection SA, New York, NY, USA). pSUPER vectors with control shRNA and shRNAs against Dlx-2 and Snail were produced and transfected as described previously (23). shRNA target sequences have also been described previously (23,29).

Immunoblotting and reverse transcription-quantitative polymerase chain reaction (RT-qPCR). Immunoblotting was performed using the following antibodies: anti-Dlx-2 (EMD Millipore, Billerica, MA, USA); anti-Snail (Abgent, San Diego, CA, USA); anti-E-cadherin, anti-COXVIIc, anti-COX15, and anti-COX19 (Santa Cruz Biotechnology, Dallas, TX, USA); anti-COXVIc, and anti-COXVIIa (MitoSciences, Eugene, OR, USA); anti-COX18 (Abcam, Cambridge, UK); anti-α-tubulin (Biogenex, Fermont, CA, USA).

Total mRNA was isolated from cells using TRIzol (Invitrogen, Carlsbad, CA, USA) according to the supplier's instructions. Transcript levels were assessed with reverse transcription-quantitative polymerase chain reaction using primers for EMT-inducing transcription factors (including Snail, Slug, Twist1, Twist2, ZEB1, ZEB2, E12/E47, Dlx-2), E-cadherin, N-cadherin, vimentin, fibronectin, cluster of differentiation 44 (CD44), COX subunits and assembly factors, and β-actin. Primer sequences described previously were used (23,29,37), along with the following additional primers: Twist1 sense, 5'-CAGACCCTCAAGCTGGCGGC-3'; Twist1 antisense, 5'-CCAGGCCCCCTCCATCCTCC-3'; Twist2 sense, 5'-TGGGCACCAGCGAGGAGGAG-3'; Twist2 antisense, 5'-CTGGGGCTGCCCTTCTTGCC-3'; ZEB1 sense, 5'-GGG AGGATGACAGAAAGGAAGG-3'; ZEB1 antisense, 5'-TGC CTCTGGTCCTCTTCAGGTGC-3'; ZEB2 sense, 5'-CAGAAG CCACGATCCAGACCGC-3'; ZEB2 antisense, 5'-GTGCCA AGGCGAGACAGCTCC-3'; E12/E47 sense, 5'-GCCGGGCAC ATGTGAAAGTAAACAA-3'; E12/E47 antisense, 5'-CAGGTT TCCACAGCATCCCCCTT-3'; N-cadherin sense, 5'-AGCCAA CCTTAACTGAGGAGT-3'; N-cadherin antisense, 5'-GGCAAG TTGATTGGAGGGATG-3'; vimentin sense, 5'-TGAAGGAGG AAATGGCTCGTC-3'; vimentin antisense, 5'-GTTTGGAAG AGGCAGAGAAATCC-3'; fibronectin sense, 5'-CAGTGGGAG ACCTCGAGAAG-3'; fibronectin antisense, 5'-TCCCTCGGA ACATCAGAAAC-3'; CD44 sense, 5'-TGCCGCTTTGCAGGT GTATT-3'; CD44 antisense, 5'-CCGATGCTCAGAGCTTTC TCC-3'. Values were normalized to those of β-actin.

Immunofluorescence (IF) staining. Cells were fixed with 3.7% formaldehyde, permeabilized in 0.2% Triton X-100, and blocked with 2% BSA. Cells were then incubated overnight with anti-E-cadherin antibody and immunostained with AlexaFluor 488-conjugated goat anti-mouse secondary antibody (Invitrogen). Hoechst 33342 (Invitrogen) was used to stain cell nuclei. Cells were viewed under a fluorescence microscope.

Chromatin immunoprecipitation (ChIP) assay. ChIP assays were performed using a ChIP assay kit (EMD Millipore) according to the manufacturer's instructions. Isotype control IgG, anti-Dlx-2, and anti-Snail (Santa Cruz Biotechnology) were used to immunoprecipitate DNA-containing complexes. ChIP-enriched DNA was analyzed by PCR using primers complementary to promoter regions containing Dlx-2 or Snail binding sites, as described previously (23,29).

Assays for mitochondrial respiration, COX activity, glucose consumption, lactate production, and ATP production. Mitochondrial respiration and COX activity were measured as described previously (23,38). For the mitochondrial respiration assay, exponentially growing cells ($1.5x10^6$) were washed with TD buffer (137 mM NaCl, 5 mM KCl, 0.7 mM Na_2HPO_4, 25 mM Tris-HCl; pH 7.4), collected, and resuspended in complete medium without phenol red. Cells ($5x10^5$) were transferred to a Mitocell chamber equipped with a Clark O_2 electrode (782 O_2 Meter; Strathkelvin Instruments, Glasgow, UK). O_2 consumption rates were measured after adding 30 μM DNP to obtain the maximum respiration rate and specificity for mitochondrial respiration was confirmed

Table I. Regulation of EMT markers and EMT-inducing transcription factors by ROS.

	H_2O_2			O_2^-		
Genes	24 h	48 h	72 h	24 h	48 h	72 h
EMT markers						
E-cadherin	0.980	0.670[b]	0.665[b]	0.963	0.496[b]	0.430[b]
N-cadherin	1.612[a]	3.382[b]	5.719[b]	1.644[b]	2.043[b]	2.135[b]
Vimentin	1.028	1.226	1.894[b]	0.975	1.537[b]	1.628[b]
Fibronectin	1.390	1.527[b]	1.945[b]	1.249	1.353	1.651[b]
CD44	1.551[b]	1.738[b]	2.034[b]	1.129	2.208[b]	2.068[b]
EMT-inducing transcription factors						
Snail	1.254	1.243	1.724[b]	1.209	2.183[b]	2.553[a]
Slug	1.210	0.835	0.940	0.935	0.705	1.080
Dlx-2	1.573[b]	1.564[b]	1.573[b]	1.615[b]	3.457[b]	2.383[b]
Twist1	1.240	1.080	1.255	1.150	1.025	1.270
Twist2	1.065	1.070	1.155	0.895	1.110	1.360
ZEB1	0.955	0.940	1.100	1.315	1.260	1.245
ZEB2	0.950	1.050	1.500	0.835	0.960	1.435
E12/E47	0.834	0.960	0.934	1.061	0.877	0.937

MCF-7 cells were treated with H_2O_2 (200 μM) or menadione (O_2^-, 10 μM) for the indicated times and then analyzed by reverse transcription-quantitative polymerase chain reaction with the indicated primers. The data were normalized against an internal control β-actin and relative expression levels were expressed as fold changes. [a]P<0.05 and [b]P<0.01 vs. untreated group. EMT, epithelial-mesenchymal transition; ROS, reactive oxygen species; CD44, cluster of differentiation 44; Dlx, distal-less; ZEB, Zinc finger E-box binding homeobox; Twist, Twist-related protein.

by adding 5 mM KCN. COX activity was determined by measuring the KCN-sensitive, COX-dependent O_2 consumption rate by adding 3 mM TMPD in the presence of 30 μM DNP and 20 μM antimycin A.

Glucose, lactate, and intracellular ATP levels in the media were determined using a glucose oxidation assay kit (Sigma-Aldrich), a colorimetric and fluorescence-based lactate assay kit (BioVision, Inc., Milpitas, CA, USA), and an ATP Bioluminescence Assay kit (Roche Diagnostics, Basel, Switzerland), respectively, according to the manufacturers' instructions. Levels of glucose, lactate, and intracellular ATP were normalized to protein concentrations. Levels of ATP produced by aerobic respiration and glycolysis were determined by measuring lactate production and O_2 consumption (23,39).

Measurement of circularity. Circularity assays were performed as described previously (29). Briefly, microscopic images were analyzed with AxioVision LE software (version 4.8). Circularity was calculated using the formula, 4π (area/perimeter^2). Values closer to 1.0 indicate a more circular cell morphology.

Statistical analysis. Reverse transcription-quantitative polymerase chain reaction, mitochondrial respiration, glucose consumption, lactate production, and ATP production assays were performed at least in triplicate. Most experiments were repeated more than twice. Data were analyzed by Student's t-test (unpaired, two-tailed) for comparison between two groups, one-way ANOVA with Tukey's multiple-comparisons test for comparison between three groups, and two-way ANOVA for comparison between three groups with multiple factors and results were expressed as mean ± SE. P<0.05 was considered to indicate a statistically significant difference.

Results and Discussion

Dlx-2/Snail cascade is implicated in ROS-induced EMT. It has been shown that ROS induces EMT by increasing Snail expression (11-14). We examined the EMT-inducing effects of H_2O_2 and O_2^- in MCF-7 cells, a non-invasive luminal A subtype breast cancer cell line. MCF-7 cells have low levels of Snail, but various stimuli including TGF and Wnt can induce Snail expression, and subsequently, EMT in MCF-7 cells; thus, MCF-7 cells are widely used for studying breast cancer, particularly EMT (40-42). ROS induced a phenotypical change to an elongated morphology with pseudopodia, which is a characteristic of mesenchymal cells, and decreased the expression of an epithelial marker, E-cadherin, indicating that ROS induce EMT (Fig. 1A and B). We further examined the effects of ROS on the expression of mesenchymal markers, such as N-cadherin, vimentin, and fibronectin. In addition, we also examined the expression of CD44, a glycoprotein receptor for various extracellular matrix (ECM) ligands, such as hyaluronic acid (HA); HA-CD44 interaction promotes EMT and CSC self-renewal through Nanog expression (43,44). ROS were shown to increase the expression of mesenchymal markers including N-cadherin, vimentin, and fibronectin (Table I and Fig. 1B). ROS also upregulated the CD44 expression (Table I and Fig. 1B). We investigated which EMT-inducing transcription factors

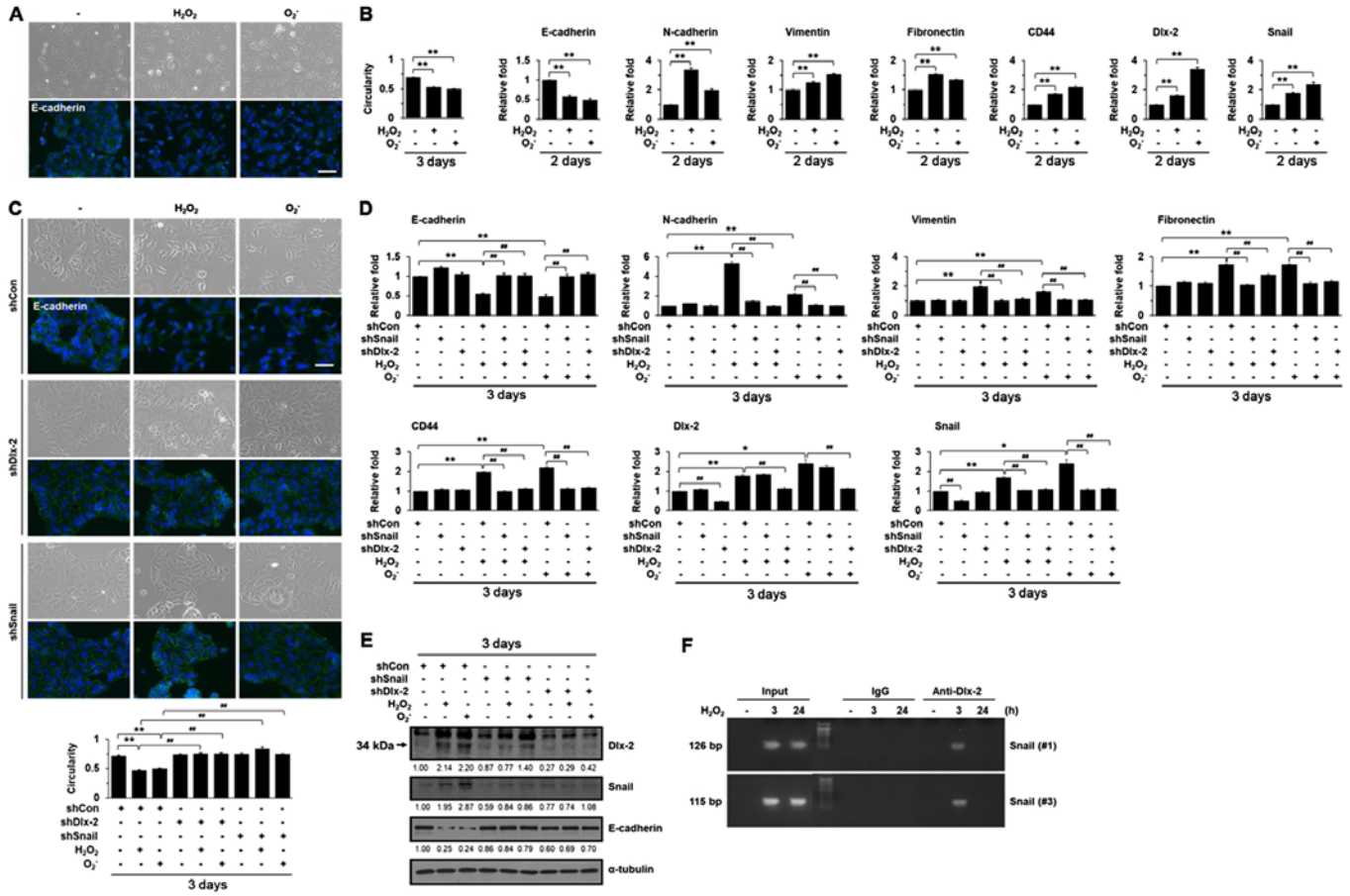

Figure 1. The Dlx-2/Snail cascade is implicated in ROS-induced EMT. (A and B) MCF-7 cells were treated with H_2O_2 (200 μM) or menadione (O_2^-; 10 μM) for 2 or 3 days. (C-E) MCF-7 cells were transfected with Dlx-2 shRNA or Snail shRNA and then treated with H_2O_2 (200 μM) or menadione (O_2^-; 10 μM) for 3 days. Cells were analyzed by phase-contrast and fluorescence microscopy for cell morphology and E-cadherin expression (fluorescence in green; left) and circularity (right). Borders were drawn along the cell edges for quantification of circularity. (A and C) Results (123-603 cells in each group) are represented as mean ± SE. (B and D) Cells were analyzed by reverse transcription-quantitative polymerase chain reaction using the indicated primers. *P<0.05 and **P<0.01 as indicated; $^{\#\#}$P<0.01 as indicated. (E) Cells were also analyzed by immunoblotting using the indicated antibodies. Quantification of the intensity of Dlx-2 and Snail bands was performed using Image J software (NIH, Bethesda, MD, USA) and normalized to the signal of tubulin. (F) MCF-7 cells were treated with H_2O_2 (200 μM) for the indicated times. ChIP assays were performed using IgG or anti-Dlx-2 antibodies and ChIP-enriched DNA was analyzed by polymerase chain reaction using primers complementary to the Dlx-2-binding region. All scale bars represent 100 μm. EMT, epithelial-mesenchymal transition; ROS, reactive oxygen species; Dlx, distal-less; ChIP, chromatin immunoprecipitation; CD44, cluster of differentiation 44.

(Snail, Slug, Twist1, Twist2, ZEB1, ZEB2, E12/E47, and Dlx-2) were involved in ROS treatment-induced EMT using reverse transcription-quantitative polymerase chain reaction (Table I). ROS induced Snail and Dlx-2 expression, but had no effect on the other EMT-inducing transcription factors (Table I and Fig. 1B). Therefore, we examined if the Dlx-2/Snail cascade was involved in ROS-induced EMT. Dlx-2 and Snail shRNAs appeared to block the EMT phenotype and downregulation of E-cadherin induced by ROS (Fig. 1C-E). We also found that Dlx-2 and Snail shRNAs prevented the ROS-induced expression of N-cadherin, vimentin, fibronectin, and CD44 (Fig. 1D). Because Dlx-2 has been shown to be an upstream regulator of Snail (29,30), we examined the effects of Dlx-2 shRNA on ROS-induced Snail expression. In the immunoblotting of Dlx-2, anti-Dlx-2 antibody recognized 2 bands (33). The lower band (indicated by arrowhead, 34 kDa) is Dlx-2; the higher band is non-specific band. Expectedly, Snail shRNA suppressed ROS-induced Snail expression and Dlx-2 shRNA suppressed ROS-induced Dlx-2 expression. In addition, Dlx-2 shRNA also prevented Snail induction by ROS, whereas Snail shRNA did not affect Dlx-2 induction by ROS (Fig. 1D and E), indicating that Dlx-2 consistently acts upstream of ROS-induced Snail. A ChIP assay showed that ROS increased Dlx-2 binding at the Snail promoter, which was detected at an early time point (3 h) after ROS treatment (Fig. 1F). Dlx-2 appeared to act as a mediator for ROS-Snail-induced EMT. These results suggest that the Dlx-2/Snail axis are implicated in ROS-induced EMT.

Dlx-2/Snail signaling is implicated in ROS-induced glycolytic switch and inhibition of mitochondrial respiration. Cancer cells exhibit glycolytic switch as well as EMT during tumor development and progression (24-28). Thus, we examined the effects of ROS on glycolytic switch and mitochondrial respiration. ROS significantly increased glucose consumption and lactate production (Fig. 2A). In addition, ROS reduced O_2 consumption (Fig. 2B). Although total ATP concentrations remained the same in all cells, ROS increased the ATP ratio produced by glycolysis versus aerobic respiration (Fig. 2C),

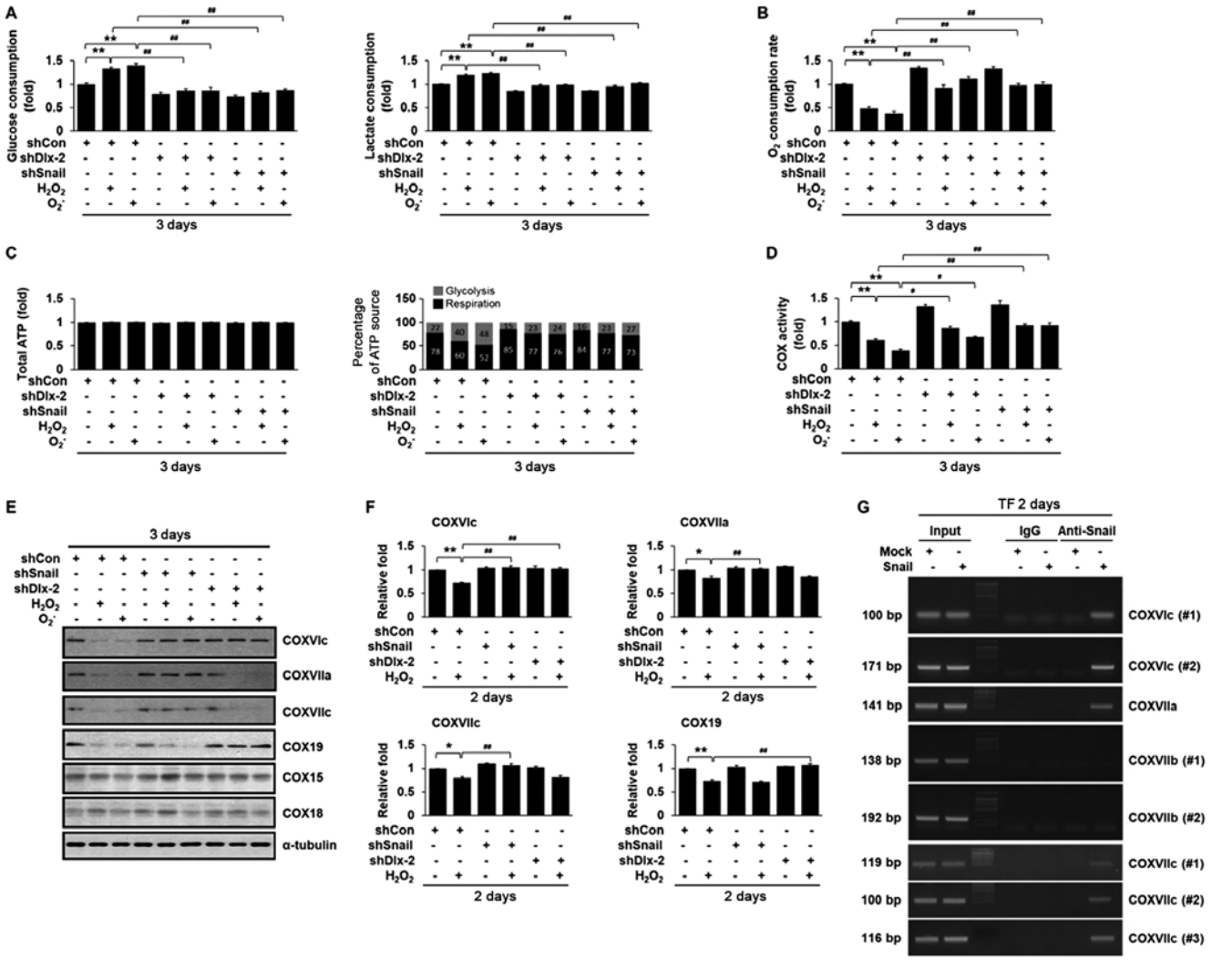

Figure 2. The Dlx-2/Snail cascade is implicated in ROS-induced glycolytic switch, inhibition of mitochondrial respiration, and COX inhibition. MCF-7 cells were transfected with Dlx-2 shRNA or Snail shRNA and treated with H_2O_2 (200 μM) or menadione (O_2^-; 10 μM) for 3 days. Cells were analyzed for (A) glucose consumption and lactate production and (B) mitochondrial respiration and (C) total ATP concentration. The amount of ATP produced by aerobic respiration (black bars) and glycolysis (gray bars) was calculated by measuring O_2 consumption and lactate production in the cells (right panels in C). (D) COX activity was measured. (E) MCF-7 cells were transfected with Dlx-2 shRNA or Snail shRNA and then treated with H_2O_2 (200 μM) or menadione (O_2^-; 10 μM) for 3 days and analyzed by immunoblotting with the indicated antibodies. (F) MCF-7 cells were transfected with Dlx-2 shRNA or Snail shRNA and then treated with H_2O_2 (200 μM) for 2 days and analyzed by real-time reverse transcription-quantitative polymerase chain reaction using the indicated primers. *P<0.05 and **P<0.01 as indicated; $^\#$P<0.05 and $^{\#\#}$P<0.01 as indicated. Bars in the graph represent mean ± SE. (G) MCF-7 cells were transfected with a Snail expression vector for 2 days. ChIP assays were performed using IgG or anti-Snail antibodies and ChIP-enriched DNA was analyzed by polymerase chain reaction using primers complementary to the Snail binding region. Dlx, distal-less; ROS, reactive oxygen species; COX, cytochrome c oxidase; ChIP, chromatin immunoprecipitation.

indicating that ROS induced glycolytic switch. Previously, we showed that the Dlx-2/Snail cascade induces glycolytic switch and inhibits mitochondrial respiration (29,30). We further examined whether the Dlx-2/Snail cascade affected ROS-induced glycolytic switch and inhibition of mitochondrial respiration. Dlx-2 and Snail shRNAs impaired the effects of ROS on glucose consumption, lactate production, and O_2 consumption (Fig. 2A-C), indicating that the Dlx-2-Snail axis is involved in ROS-induced glycolytic switch and inhibition of mitochondrial respiration.

Dlx-2/Snail signaling is implicated in ROS-induced COX activity repression. Inhibition of mitochondrial respiratory activity is closely related to changes in the activity of COX, the terminal enzyme of the mitochondrial respiratory chain. We found that ROS repressed COX activity (Fig. 2D). Thus, we further examined the involvement of the Dlx-2/Snail cascade in ROS-induced downregulation of COX activity. Dlx-2 and Snail shRNAs suppressed ROS-induced downregulation of COX activity (Fig. 2D), implicating the Dlx-2/Snail cascade in ROS-induced COX activity repression.

Dlx-2/Snail signaling is implicated in ROS-induced COX activity repression by downregulating multiple COX subunits and assembly factors. Eukaryotic COX is composed of 13 different subunits in the inner mitochondrial membrane and the sequential action of several assembly factors regulates its assembly (Table II). We further examined the effects of ROS on the expression of COX subunits and assembly factors. ROS downregulated the expression of COXVIc, COXVIIa, COXVIIc, COX15, COX18, and COX19 (Table II). Note that ROS decreased the

Table II. Regulation of gene expression of COX subunits and assembly factors by ROS.

	H_2O_2 (n=2-3)	O_2^- (n=4)
Genes	48 h	48 h
COX subunits		
COXIV	1.067	1.138
COXVa	1.047	1.018
COXVb	0.978	1.214
COXVIa	1.021	1.047
COXVIb	0.853	1.425
COXVIc	0.728[b]	0.704[b]
COXVIIa	0.826[b]	0.431[b]
COXVIIb	1.188	1.045
COXVIIc	0.804[a]	0.778[b]
COXVIII	1.072	1.053
Assembly factors		
COX10	0.942	0.918
COX11	1.103	1.028
COX15	0.776[a]	0.653[b]
COX17	1.016	0.939
COX18	0.836[a]	0.865[b]
COX19	0.742[b]	0.849[b]
LRPPRC	1.139	1.051
SURF1	0.773	1.274
SCO1	1.036	1.170
SCO2	1.058	1.055

MCF-7 cells were treated with H_2O_2 (200 μM) or menadione (O_2^-, 10 μM) for 48 h and then analyzed by reverse transcription-quantitative polymerase chain reaction with the indicated primers. The data were normalized against an internal control β-actin and relative expression levels were expressed as fold changes. [a]P<0.05; [b]P<0.01 vs. untreated group. COX, cytochrome c oxidase; LRPPRC, leucine-rich pentatricopeptide repeat-containing protein; SCO, synthesis of cytochrome c oxidase; SURF1, surfeit locus protein 1; ROS, reactive oxygen species.

mRNA levels of COX15 and COX18, but not their protein levels (Fig. 2E and F; Table II). We previously found that Snail decreased expression of COXVIc, COXVIIa, and COXVIIc (23) and Dlx-2 decreased expression of COXVIc and COX19 (29). Snail shRNA suppressed the ROS-induced reduction in the levels of COXVIc, COXVIIa, and COXVIIc, but not COX19 (Fig. 2E and F). Dlx-2 shRNA suppressed the ROS-induced reduction in the levels of COXVIc and COX19, but not COXVIIa and COXVIIc (Fig. 2E and F).

Several Snail-binding sites (E-box) were previously found in the promoters of COX subunits (23). To examine whether the expression of the COX subunits was regulated by Snail, we conducted a ChIP assay. Snail bound to the COXVIc, COXVIIa, and COXVIIc promoters (Fig. 2G), which is consistent with previous observations (23). Among the COX subunits, COXVIc acted as a common target of ROS, Dlx-2, and Snail. Therefore, COXVIc may play an important role in the repression of COX activity via the ROS-Dlx-2/Snail-mediated pathway. For judging the transformation of the proteome accurately, the proteome needs to be analyzed by mass spectrometry-based methods, such as liquid chromatography time-of-flight mass spectrometry (LC-TOF-MS), ultra-performance liquid chromatography triple quadrupole mass spectrometry (UPLC-TQ-MS), and gas chromatography time-of-flight mass spectrometry (GC-TOF-MS), together with bioinformatics analyses (45,46). Thus, proteome transformation is yet to be examined in further studies, but cumulatively, our findings suggest that the ROS-Dlx-2/Snail axis plays a crucial role in breast tumor progression by regulating EMT, mitochondrial repression, and glycolytic switch.

NF-κB has been shown to be involved in ROS-induced EMT (13). NF-κB induces EMT-inducing transcription factors such as Snail, Slug, ZEB1, ZEB2, and Twist; NF-κB/p65 transcriptionally regulates the expression of these transcription factors, which in turn represses the epithelial marker E-cadherin and activates the mesenchymal marker N-cadherin, thereby resulting in the induction of EMT (47-49). Additionally, NF-κB stimulates the expression of HIF-1α, also contributing to EMT (48). Furthermore, NF-κB activation induces matrix-degrading enzymes such as MMP9, thus contributing to EMT (50). NF-κB is known to be involved in ROS-induced EMT via Snail induction (13). Because we found that ROS induce EMT through the Dlx-2/Snail cascade, we think that an interplay between NF-κB and Dlx-2 may possibly exist for Snail activation in ROS-induced EMT; this interplay between NF-κB and Dlx-2 is yet to be elucidated in further studies.

It has been shown that ROS are involved in many aspects of cellular signaling. TGF-β1 has been shown to activate the ROS-NFκB pathway, which plays an important role in TGF-β1-induced EMT, cell migration, and invasion (51). We have also shown that Dlx-2/Snail signaling is involved in TGF-β-induced EMT (29,30). Thus, the ROS-Dlx-2/Snail cascade may be involved in TGF-β-induced EMT. In addition, it was recently reported that ROS are involved in EMT and cancer metastasis induced by chemotherapeutics, such as 5-fluorouracil (5-FU), gemcitabine (GEM), and oxaliplatin (52-54). EMT contributes to chemoresistance in cancer cells. Dual oxidase 2 (DUOX2)-induced ROS promote the induction of EMT in 5-FU-resistant colon cancer cells (52). In addition, in GEM-treated pancreatic ductal adenocarcinoma (PDAC) patients, the levels of glutathione peroxidase-1 (GPx1), an antioxidant enzyme, are negatively regulated. GPx1 inhibits ROS-mediated Akt/GSK3β/Snail signaling, thereby suppressing EMT and chemoresistance in PDAC (53). ROS have been shown to mediate oxaliplatin-induced EMT and invasive potential in colon cancer (54). Our results suggest that ROS-induced Dlx-2/Snail signaling may be involved in EMT and may be induced by these chemotherapeutics. Note that we used only one cell line in this study, thus our results are limited to MCF-7 cells. Therefore, the Dlx-2/Snail axis is a potential therapeutic target for the prevention of metastasis and tumor progression in MCF-7 cells; this mechanism may be the case for breast cancer in general.

Acknowledgements

Not applicable.

Funding

This study was supported by the National Research Foundation of Korea (NRF) grant funded by the Korean government (MSIP) (grant nos. 2015M2B2A9028108, 2015R1A2A2A01004468, 2017R1A2B4010411 and 2017R1A6A3A11030673).

Availability of data and materials

All data generated or analyzed during this study are included in this published article.

Authors' contributions

SYL, MKJ, HMJ and HSK conceived and designed the project. SYL, MKJ and HMJ performed the experiments. SYL, MKJ, HMJ, CHK, HGP, SIH, YJL and HSK analyzed and interpreted the data. SYL, MKJ, HMJ, YJL and HSK wrote the manuscript. HSK supervised the project. All authors read and approved the final manuscript.

Ethics approval and consent to participate

Not applicable.

Patient consent for publication

Not applicable.

Competing interests

The authors declare that they have no competing interests.

References

1. Storz P: Reactive oxygen species in tumor progression. Front Biosci 10: 1881-1896, 2005.
2. Liou GY and Storz P: Reactive oxygen species in cancer. Free Radic Res 44: 479-496, 2010.
3. Schieber M and Chandel NS: ROS function in redox signaling and oxidative stress. Curr Biol 24: R453-R462, 2014.
4. Mittler R: ROS Are Good. Trends Plant Sci 22: 11-19, 2017.
5. Di Meo S, Reed TT, Venditti P and Victor VM: Harmful and beneficial role of ROS. Oxid Med Cell Longev 2016: 7909186, 2016.
6. Wu WS: The signaling mechanism of ROS in tumor progression. Cancer Metastasis Rev 25: 695-705, 2006.
7. de Sá Junior PL, Câmara DAD, Porcacchia AS, Fonseca PMM, Jorge SD, Araldi RP and Ferreira AK: The roles of ROS in cancer heterogeneity and therapy. Oxid Med Cell Longev 2017: 2467940, 2017.
8. Zorov DB, Juhaszova M and Sollott SJ: Mitochondrial reactive oxygen species (ROS) and ROS-induced ROS release. Physiol Rev 94: 909-950, 2014.
9. Han D, Williams E and Cadenas E: Mitochondrial respiratory chain-dependent generation of superoxide anion and its release into the intermembrane space. Biochem J 353: 411-416, 2001.
10. Burdon RH: Superoxide and hydrogen peroxide in relation to mammalian cell proliferation. Free Radic Biol Med 18: 775-794, 1995.
11. Cannito S, Novo E, di Bonzo LV, Busletta C, Colombatto S and Parola M: Epithelial-mesenchymal transition: from molecular mechanisms, redox regulation to implications in human health and disease. Antioxid Redox Signal 12: 1383-1430, 2010.
12. Pani G, Giannoni E, Galeotti T and Chiarugi P: Redox-based escape mechanism from death: the cancer lesson. Antioxid Redox Signal 11: 2791-2806, 2009.
13. Cichon MA and Radisky DC: ROS-induced epithelial-mesenchymal transition in mammary epithelial cells is mediated by NF-kB-dependent activation of Snail. Oncotarget 5: 2827-2838, 2014.
14. Lim SO, Gu JM, Kim MS, Kim HS, Park YN, Park CK, Cho JW, Park YM, Jung G: Epigenetic changes induced by reactive oxygen species in hepatocellular carcinoma: methylation of the E-cadherin promoter. Gastroenterology 135: 2128-2140, 2140 e2121-2128, 2008.
15. De Craene B and Berx G: Regulatory networks defining EMT during cancer initiation and progression. Nat Rev Cancer 13: 97-110, 2013.
16. Tsai JH and Yang J: Epithelial-mesenchymal plasticity in carcinoma metastasis. Genes Dev 27: 2192-2206, 2013.
17. Puisieux A, Brabletz T and Caramel J: Oncogenic roles of EMT-inducing transcription factors. Nat Cell Biol 16: 488-494, 2014.
18. Micalizzi DS, Farabaugh SM and Ford HL: Epithelial-mesenchymal transition in cancer: Parallels between normal development and tumor progression. J Mammary Gland Biol Neoplasia 15: 117-134, 2010.
19. Iwatsuki M, Mimori K, Yokobori T, Ishi H, Beppu T, Nakamori S, Baba H and Mori M: Epithelial-mesenchymal transition in cancer development and its clinical significance. Cancer Sci 101: 293-299, 2010.
20. Peinado H, Olmeda D and Cano A: Snail, Zeb and bHLH factors in tumour progression: an alliance against the epithelial phenotype? Nat Rev Cancer 7: 415-428, 2007.
21. Wang Y, Shi J, Chai K, Ying X and Zhou BP: The role of snail in EMT and tumorigenesis. Curr Cancer Drug Targets 13: 963-972, 2013.
22. De Craene B, Denecker G, Vermassen P, Taminau J, Mauch C, Derore A, Jonkers J, Fuchs E and Berx G: Epidermal snail expression drives skin cancer initiation and progression through enhanced cytoprotection, epidermal stem/progenitor cell expansion and enhanced metastatic potential. Cell Death Differ 21: 310-320, 2014.
23. Lee SY, Jeon HM, Ju MK, Kim CH, Yoon G, Han SI, Park HG and Kang HS: Wnt/Snail signaling regulates cytochrome C oxidase and glucose metabolism. Cancer Res 72: 3607-3617, 2012.
24. Warburg O: On the origin of cancer cells. Science 123: 309-314, 1956.
25. Hsu PP and Sabatini DM: Cancer cell metabolism: Warburg and beyond. Cell 134: 703-707, 2008.
26. Vander Heiden MG, Cantley LC and Thompson CB: Understanding the Warburg effect: the metabolic requirements of cell proliferation. Science 324: 1029-1033, 2009.
27. Cairns RA, Harris IS and Mak TW: Regulation of cancer cell metabolism. Nat Rev Cancer 11: 85-95, 2011.
28. Finley LW, Zhang J, Ye J, Ward PS, Thompson CB: SnapShot: cancer metabolism pathways. Cell Metab 17: 466-466 e462, 2013.
29. Lee SY, Jeon HM, Ju MK, Jeong EK, Kim CH, Yoo MA, Park HG, Han SI and Kang HS: Dlx-2 is implicated in TGF-β- and Wnt-induced epithelial-mesenchymal, glycolytic switch, and mitochondrial repression by Snail activation. Int J Oncol 46: 1768-1780, 2015.
30. Lee SY, Jeon HM, Ju MK, Jeong EK, Kim CH, Park HG, Han SI and Kang HS: Dlx-2 and glutaminase upregulate epithelial-mesenchymal transition and glycolytic switch. Oncotarget 7: 7925-7939, 2016.
31. Merlo GR, Zerega B, Paleari L, Trombino S, Mantero S and Levi G: Multiple functions of Dlx genes. Int J Dev Biol 44: 619-626, 2000.
32. Panganiban G and Rubenstein JL: Developmental functions of the Distal-less/Dlx homeobox genes. Development 129: 4371-4386, 2002.
33. Lee SY, Jeon HM, Kim CH, Ju MK, Bae HS, Park HG, Lim SC, Han SI and Kang HS: Homeobox gene Dlx-2 is implicated in metabolic stress-induced necrosis. Mol Cancer 10: 113, 2011.
34. Yilmaz M, Maass D, Tiwari N, Waldmeier L, Schmidt P, Lehembre F and Christofori G: Transcription factor Dlx2 protects from TGFβ-induced cell-cycle arrest and apoptosis. EMBO J 30: 4489-4499, 2011.
35. Tang P, Huang H, Chang J, Zhao GF, Lu ML and Wang Y: Increased expression of DLX2 correlates with advanced stage of gastric adenocarcinoma. World J Gastroenterol 19: 2697-2703, 2013.

36. Yan ZH, Bao ZS, Yan W, Liu YW, Zhang CB, Wang HJ, Feng Y, Wang YZ, Zhang W, You G, *et al*: Upregulation of DLX2 confers a poor prognosis in glioblastoma patients by inducing a proliferative phenotype. Curr Mol Med 13: 438-445, 2013.
37. Kim CH, Jeon HM, Lee SY, Ju MK, Moon JY, Park HG, Yoo MA, Choi BT, Yook JI, Lim SC, et al: Implication of snail in metabolic stress-induced necrosis. PLoS One 6: e18000, 2011.
38. Yoon YS, Lee JH, Hwang SC, Choi KS and Yoon G: TGF beta1 induces prolonged mitochondrial ROS generation through decreased complex IV activity with senescent arrest in Mv1Lu cells. Oncogene 24: 1895-1903, 2005.
39. Sariban-Sohraby S, Magrath IT and Balaban RS: Comparison of energy metabolism in human normal and neoplastic (Burkitt's lymphoma) lymphoid cells. Cancer Res 43: 4662-4664, 1983.
40. Dong C, Yuan T, Wu Y, Wang Y, Fan TW, Miriyala S, Lin Y, Yao J, Shi J, Kang T, et al: Loss of FBP1 by Snail-mediated repression provides metabolic advantages in basal-like breast cancer. Cancer Cell 23: 316-331, 2013.
41. Jin L, Zhu C, Wang X, Li C, Cao C, Yuan J and Li S: Urocortin attenuates TGFβ1-induced Snail1 and slug expressions: inhibitory role of Smad7 in Smad2/3 signaling in breast cancer cells. J Cell Biochem 116: 2494-2503, 2015.
42. Rios Garcia M, Steinbauer B, Srivastava K, Singhal M, Mattijssen F, Maida A, Christian S, Hess-Stumpp H, Augustin HG, *et al*: Acetyl-CoA carboxylase 1-dependent protein acetylation controls breast cancer metastasis and recurrence. Cell Metab 26: 842-855 e845, 2017.
43. Xu H, Tian Y, Yuan X, Wu H, Liu Q, Pestell RG and Wu K: The role of CD44 in epithelial-mesenchymal transition and cancer development. Onco Targets Ther 8: 3783-3792, 2015.
44. Chanmee T, Ontong P, Kimata K and Itano N: Key roles of hyaluronan and Its CD44 receptor in the stemness and survival of cancer stem cells. Front Oncol 5: 180, 2015.
45. Han X, Aslanian A and Yates JR III: Mass spectrometry for proteomics. Curr Opin Chem Biol 12: 483-490, 2008.
46. Dettmer K, Aronov PA and Hammock BD: Mass spectrometry-based metabolomics. Mass Spectrom Rev 26: 51-78, 2007.
47. Min C, Eddy SF, Sherr DH and Sonenshein GE: NF-kappaB and epithelial to mesenchymal transition of cancer. J Cell Biochem 104: 733-744, 2008.
48. Taniguchi K and Karin M: NF-κB, inflammation, immunity and cancer: Coming of age. Nat Rev Immunol 18: 309-324, 2018.
49. Pires BR, Mencalha AL, Ferreira GM, de Souza WF, Morgado-Díaz JA, Maia AM, Corrêa S and Abdelhay ES: NF-kappaB is involved in the regulation of EMT genes in breast cancer cells. PLoS One 12: e0169622, 2017.
50. Huang S, Pettaway CA, Uehara H, Bucana CD and Fidler IJ: Blockade of NF-kappaB activity in human prostate cancer cells is associated with suppression of angiogenesis, invasion, and metastasis. Oncogene 20: 4188-4197, 2001.
51. Tobar N, Villar V and Santibanez JF: ROS-NFkappaB mediates TGF-beta1-induced expression of urokinase-type plasminogen activator, matrix metalloproteinase-9 and cell invasion. Mol Cell Biochem 340: 195-202, 2010.
52. Kang KA, Ryu YS, Piao MJ, Shilnikova K, Kang HK, Yi JM, Boulanger M, Paolillo R, Bossis G, Yoon SY, *et al*: DUOX2-mediated production of reactive oxygen species induces epithelial mesenchymal transition in 5-fluorouracil resistant human colon cancer cells. Redox Biol 17: 224-235, 2018.
53. Meng Q, Shi S, Liang C, Liang D, Hua J, Zhang B, Xu J and Yu X: Abrogation of glutathione peroxidase-1 drives EMT and chemoresistance in pancreatic cancer by activating ROS-mediated Akt/GSK3β/Snail signaling. Oncogene 37: 5843-5857, 2018.
54. Jiao L, Li DD, Yang CL, Peng RQ, Guo YQ, Zhang XS and Zhu XF: Reactive oxygen species mediate oxaliplatin-induced epithelial-mesenchymal transition and invasive potential in colon cancer. Tumour Biol 37: 8413-8423, 2016.